J Neural Transm (1997) 104: 161–173

Journal of Neural Transmission

Prestimulus EEG microstates influence visual event-related potential microstates in field maps with 47 channels

I. Kondakor[1,2,*], **D. Lehmann**[1,2], **C. M. Michel**[2,3], **D. Brandeis**[4], **K. Kochi**[1], and **T. Koenig**[1]

[1]The KEY Institute for Brain-Mind Research, University Hospital of Psychiatry, and [2]EEG-EP Mapping Laboratory, Department of Neurology, University Hospital, Zurich, [3]Laboratoire de Cartographie des Fonctions Cerebrales, Department of Neurology, University Hospital, Geneva, and [4]Department of Child and Adolescent Psychiatry, University of Zurich, Zurich, Switzerland

Accepted December 18, 1996

Summary. The influence of the immediate prestimulus EEG microstate (sub-second epoch of stable topography / map landscape) on the map landscape of visually evoked 47-channel event-related potential (ERP) microstates was examined using the frequent, non-target stimuli of a cognitive paradigm (12 volunteers). For the two most frequent prestimulus microstate classes (oriented left anterior-right posterior and right anterior-left posterior), ERP map series were selectively averaged. The post-stimulus ERP grand average map series was segmented into microstates; 10 were found. The centroid locations of positive and negative map areas were extracted as landscape descriptors. Significant differences (MANOVAs and t-tests) between the two prestimulus classes were found in four of the ten ERP microstates. The relative orientation of the two ERP microstate classes was the same as prestimulus in some ERP microstates, but reversed in others. – Thus, brain electric microstates at stimulus arrival influence the landscapes of the post-stimulus ERP maps and therefore, information processing; prestimulus microstate effects differed for different post-stimulus ERP microstates.

Keywords: ERP microstates, event-related potential maps, state-dependency of ERP maps, prestimulus EEG microstate, visual odd-ball paradigm.

Introduction

It is clear that all information processing in the brain depends on the momentary functional state of the brain: different outputs occur to identical inputs,

*Present address: Department of Neurology, Medical School, University of Pécs, H-7623 Pécs, Rét u. 2, Hungary

depending, for instance, on maturation level, motivation, vigilance, attention, selective attention as well as metabolic and disease conditions, and psychoactive drugs. The functional state of the human brain is very sensitively reflected by its electrical activity, i.e., by the spontaneous electroencephalogram (EEG) or the event-related potentials (ERPs) as reported in many papers (e.g., Koukkou and Lehmann, 1968, 1983; John et al., 1988). Different ERP waveforms have been observed depending on the factors mentioned above (e.g., Chourchesne, 1978; Friedman et al., 1990; Koelega and Verbaten, 1991; Takeda et al., 1992; Michel and Lehmann, 1993; Näätänen et al., 1993; Woods, 1993).

More specifically, a number of studies using various approaches showed that the waveform of event-related potentials to an incoming stimulus depends on the EEG waveform during a finite time epoch concurrent with or immediately preceding the stimulus (Corletto et al., 1967; Basar, 1980; Basar et al., 1984; Gath et al., 1983, 1985; Romani et al., 1988, 1991; Rahn and Basar, 1993). The waveform approaches used in these studies naturally require an epoch of a certain minimum duration, typically one or more seconds, to classify the prestimulus waveform; further, the approaches examine local features of the brain electric field, typically sequences of potential differences between two electrode sites.

The brain is a complex, dynamic, and state-dependent system which is adaptively regulated and homeostatically stable (Ashby, 1960). Thus, depending on the functional state at input arrival, the response may differ, but it will be within physiological constraints. The entire brain can be said to be in a particular state at each moment in time, however many constituting subprocesses participate (Ashby, 1960). This concept is operationalized by assessing the momentary spatial configurations of the space-extended brain electric field (Lehmann, 1987). At each moment in time, the field represents the sum of all momentary, local brain processes. Different spatial configurations or landscapes of the field must have been caused by the activity of different neural generators, thus reflecting the execution of different brain functions. This approach implies a virtually unlimited time resolution (time-sample-by-time-sample decisions) and is therefore most appropriate for studies on brain information processing because these latter operations occur in the millisecond to sub-second range. Several studies on spontaneous (Lehmann et al., 1987; Wackermann et al., 1993; Kinoshita et al., 1995) as well as event-related data (Lehmann and Skrandies, 1980; Brandeis et al., 1995; Pascual-Marqui et al., 1995; Koenig and Lehmann, 1996) showed that the field configuration changes in a clearly discontinuous way within a sub-second time range: brief epochs of quasi-stable field topography are concatenated by rapid changes of the spatial configuration. Algorithms that parse the sequences of momentary field maps into time segments of stable topography reduce these map series into sequences of microstates. In a study with an auditory P300 paradigm, we found that the last prestimulus EEG microstate influenced the maps of conventionally defined, subsequent ERP components to the frequent stimuli (Lehmann et al., 1994). The utilized, most frequent two classes of prestimulus microstates had diagonal field orientations with crossed directions. The three

examined ERP components covered only parts of the post-stimulus epoch, but all three showed the same orientation difference, that of the prestimulus microstates, thus suggestive of a simple, long lasting persistence of the field type.

The present study investigated the question whether a comprehensive analysis of the ERP map series using microstate segmentation will detect prestimulus-dependent ERP microstate maps that do not show persisting prestimulus differences as well as microstates that do. It further tested the hypothesis that the influence of the prestimulus EEG microstate is independent of stimulus modality and experimental paradigm. Non-target, frequent stimuli in a cognitive, visual paradigm were analysed. A pilot analysis of the data had used successive ERP map comparisons (Kondakor et al., 1995) and found prestimulus map-depending differences. The present study extended this work within the conceptual framework of ERP microstate segmentation.

Methods

Subjects

Twelve normal healthy male volunteers between 20 and 33 years were recruited as paid subjects. They were not pre-screened for EEG or ERP patterns. All subjects were right-handed as tested with the Edinburgh handedness 12-items inventory (Oldfield, 1970).

Experimental setup

The subjects were engaged in a visual information processing task of the "oddball paradigm"-type. They observed single digits appearing on a screen in a pseudo-random order, and they were requested to press a microswitch whenever the last three digits were either odd or even ("triplets"; Michel and Lehmann, 1993). The single digits subtended 1.5 degrees visual angle, and were presented at intervals of 704 ms; each was shown for 100 ms duration.

Having been instructed about the task, the subject was seated in a comfortable chair in a sound-, light-, and electrically shielded room. During a recording session, 20 recording runs were done, each lasting about 2 min and including about 170 stimuli; 13–16 triplets occurred in each run. There were breaks of 1 min after each run. All subjects had two recording sessions separated by at least one week, one with placebo and one with a drug (2 mg Valium^{R}) in a double-blind cross-over design. The subjects' questionaire reports on subjective estimates of possible drug effects showed no significant subjective drug effect of the placebo sessions. The placebo data were used for the present analysis.

Recordings

Forty-seven electrodes were attached to the scalp covering the head from 20 to 100% of the nasion-inion and 10–90% of the left-right distance of the 10/20 system at about equidistant spacing, and recorded vs Cz. Impedances were below 10 kOhm. Additional channels recorded the stimulus sequence, and the bipolar EOG from electrodes above the right and below the left eye. Recording was done (bandpass 0.1–40 Hz) using a 64-channel amplifier system by M & I (Prague, Czechia), an A/D converter system (1024 samples/sec/channel) by Burr-Brown and acquisition/display software by Neuroscience Technology Research (Prague, Czechia). Off-line, the data were downsampled to 256 Hz and temporally filtered with a digital FIR low pass filter (25 Hz). Spatial DC offset was removed for each time frame ("average reference" computation, Offner, 1950). Stimulus epochs were formed that covered the time from 156 ms before until 700 ms after each stimulus (40 plus

180 time frames). An artifact identification routine was applied that identified all stimulus epochs with signal amplitudes higher than 100 μ V in any channel for subsequent manual artifact rejection.

Analyzed data

Only those stimuli were used which are expected to elicit similar and relatively simple cognitive processing without specific anticipations such as represented by the contingent negative variation (McCallum, 1988) and without responses to occurrences or non-occurrences of expected targets ("update", "closure", "mismatch"; Kutas and Hillyard, 1980; Picton, 1992; Michel and Lehmann, 1993). Within the series of the presented odd (O) or even (E) digit stimuli, a new stimulus may (1) follow an O-E- or E-O- sequence. If the new stimulus was (1a) of the opposite type to the last stimulus, it started a new sequence and was accepted. If the new stimulus was (1b) of the same type as the last one, it set the scene to expect a completion of a target (triplet) sequence by the subsequent stimulus; since we wished to avoid cases of specific expectancy, (1b) stimuli were excluded. Alternatively, the new stimulus may (2) follow an E-E- or O-O-sequence where it may or may not complete a target triplet. In either case it was excluded, since (2a) a new stimulus of the opposite type was a mismatch and (2b) a new stimulus of the same type was a target completion.

The mean number of qualifying stimulus epochs, after artifact editing, was 1553/subject.

Classes of prestimulus microstates

The momentary brain electric microstate that existed when a stimulus occurred was classified following the original microstate segmentation procedure (Lehmann et al., 1987). The time moments of maximal field strength (Global Field Power, Lehmann and Skrandies, 1980) and thus, optimal signal to noise ratio were used for classification according to their map topography. Global Field Power was computed as the standard deviation of all measured potential values in the map, corresponding to the effective field value, and representing the strength of the momentary field. For each prestimulus epoch, this was calculated for each of the 40 time frames before the stimulus. The values were searched backwards from the stimulus, to identify the map at the last maximal value of Global Field Power before the stimulus. The maps at these maximal strength times were selected for classifications of the prestimulus microstates.

The topography of the landscape of each selected map was assessed by the locations of its two extreme potential values (minimum and maximum). The locations of these two extremes were coded as left-right and anterior-posterior electrode positions in the schematized array (Fig. 1A). The polarity of the extremes is disregarded, because a microstate in spontaneous EEG is conceived as consisting of a string of repeated polarity reversals of a stable map landscape (Lehmann et al., 1987) in agreement with the analysis approaches for spontaneous EEG where spectral power and coherence are used to assess brain macrostates. Theoretically, the number of the possible pairs of extreme locations, i.e. of different classes of microstates is 47*46/2 = 1081 for 47 electrodes.

We wanted to compare the effect of two prestimulus classes of microstates on their post-stimulus ERP maps. The two classes should be maximally different in terms of topography. In order to average a sufficient number of stimuli, different possible types of prestimulus microstate classes were defined and examined for frequency of occurrence. It is known from earlier studies that the most frequent microstate landscapes tend to be oriented generally in the anterior-posterior direction, with a diagonal left or right tendency (Lehmann, 1971; Lehmann et al., 1994). Accordingly, the recorded electrode array was divided into its four quadrants (Fig. 1B). Of the total of 1553 available frequent stimuli on the average for each subject, 267 cases had both extremes of the prestimulus microstate in the same quadrant and thus were not of interest for clearly defined maximal

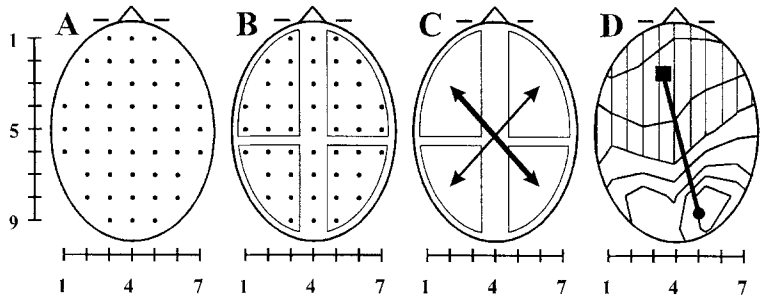

Fig. 1. **A** Recording array; the dots indicate the electrode locations; row numbering from anterior to posterior, column numbering from left to right. **B** The quadrants of the recording area. **C** The two most frequently occurring prestimulus microstate classes, where the extrema were in the left-anterior and right-posterior quadrants (class I, heavy line), and in the right-anterior and left-posterior quadrants (class II, thin line). **D** Example of a momentary potential distribution map (an equipotential contour-line map) with the locations of the centroids of the positive (white) and negative (hatched) map areas drawn in and connected by a line; round symbol = positive centroid, square symbol = negative centroid

differences of landscapes. Another 494 stimuli per subject involved midline electrodes and oblique combinations where the extremes were at anterior-posterior neighbor electrode rows, thus presenting ambivalence in assignment or weak differences in landscape (near horizontal field orientations with minimal centroid distance). After omission of these cases, 792 stimuli/subject remained; these cases formed the transverse, sagittal and diagonal combinations of the quadrants. In 97 stimuli/subject, the extreme pairs transversely combined the anterior left and right quadrants (actual occurrence probability 1.3% below expectation), and in 77 stimuli/subject the posterior left and right quadrants (6.1% below expectation, $p < 0.002$). In 97 stimuli/subject the extremes combined sagittaly the left anterior and posterior quadrants (actual occurrence probability 3.6% below expectation, $p < 0.04$), and in 115 stimuli/subject, the right anterior and posterior quadrants (actual occurrence probability 1% below expectation). In 212 stimuli/subject (SD = 50.2) the extreme values were diagonally in the left anterior and right posterior quadrants, and in 194 (SD = 51.8) the extreme values were diagonally in the right anterior and left posterior quadrants. The stimuli in these later two classes occurred at 8.1% and 5.6% above the expected chance levels ($p < 0.003$ and 0.008, respectively).

These latter two types of microstate classes with diagonal orientations of their field axes were used for the final analysis. The prestimulus microstate type with the left anterior-right posterior orientation of the field axis was called class I (on the average, 212 stimuli/subject), that with the right anterior-left posterior type, class II (on the average, 194 stimuli/subject), as illustrated in Fig. 1C.

For each subject, all post-stimulus epochs belonging to the two prestimulus classes I and II were averaged separately. Thus, for each prestimulus class there were 12 average ERP map series covering 700 ms post-stimulus.

Parsing the post-stimulus ERP map series into microstates

The grand mean ERP map series calculated across all subjects and both prestimulus classes was segmented into microstates, i.e. time epochs of the map series characterized by quasi-stable map landscapes (Lehmann, 1987; Koenig and Lehmann, 1996). The segmentation strategy used the sequential computation of Global Map Dissimilarity for all successive pairs of maps of the map series (Lehmann and Skrandies, 1980; Lehmann, 1987). The resulting function was smoothed with a FIR low-pass filter set to 25 Hz (i.e.,

identical with the FIR low-pass applied to the data) and yielded the profile shown in Fig. 2A. The microstate borders, i.e. the time points of maximal dissimilarity between successive maps, were found at the post-stimulus times listed in Table 1. Table 1 also lists the varying microstate durations. Independently parsing the mean map series (across subjects) of the two prestimulus classes yielded dissimilarity curves that showed peaks within +/− 1 time frame of the grand mean curve combining both prestimulus classes (Fig. 2C and 2D).

Another approach to the segmentation of ERP map series into microstates uses a similarity criterion which all member maps of a microstate have to fulfil. If this criterion is applied to the map series in a sequential mode, a time function of the probability of the occurrence of microstate borders across all magnitudes of the criterion is computed (Koenig, 1995). We used as criterion all possible different spatial window sizes around the locations of the centroids of the positive and negative areas of the map (Fig. 2B).

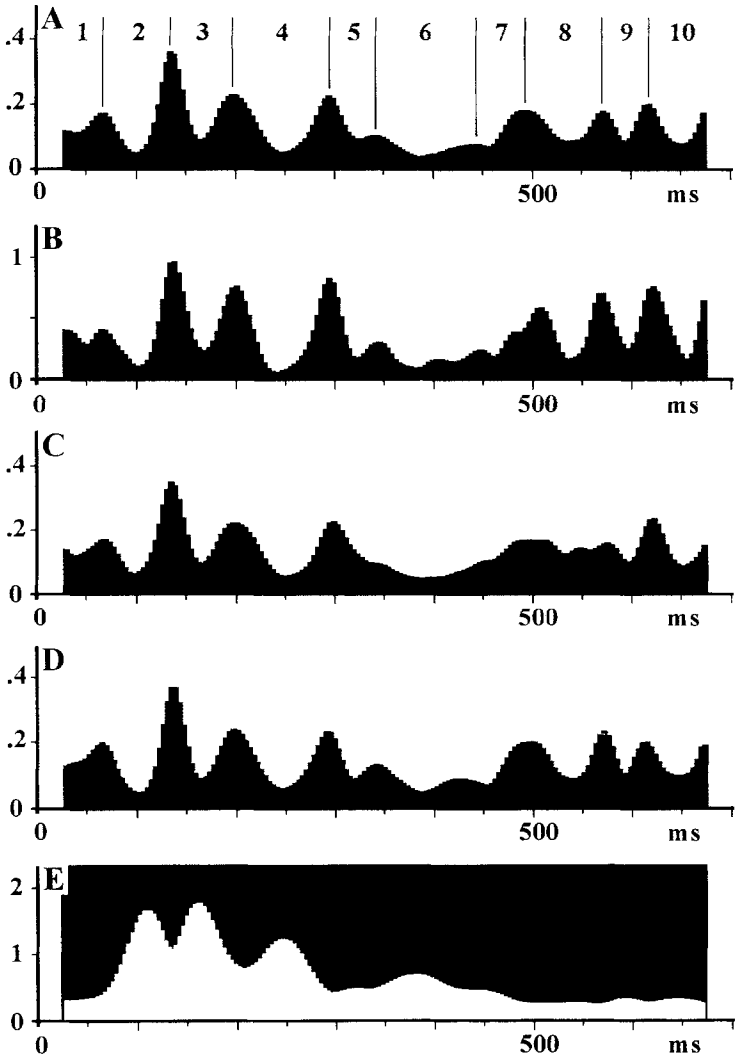

Fig. 2. **A** Global Map Dissimilarity of the grand mean ERP map series. **B** Microstate Border Probability of same data as in A. **C** Global Map Dissimilarity of the grand mean ERP data of prestimulus class I. **D** Global Map Dissimilarity of the grand mean ERP data of prestimulus class II. **E** Global Field Power of same data as in A

Although this approach considers the similarity of all maps of each microstate, the resulting probability function covaries almost exactly with the Global Map Dissimilarity curve (see also Koenig, 1995) which examined pairs of successive maps for maximal dissimilarity (Fig. 2A).

Still another independent measure, the momentary global field strength (Global Field Power, Lehmann and Skrandies, 1980) computed as function of time produced minimal values at time points of maximal Global Map Dissimilarity (compare Fig. 2E vs. 2A), confirming the reported high correlation between these two computationally independent measures (Lehmann and Skrandies, 1980) that can be used to identify microstates.

Comparing ERP microstates between conditions

Mean maps were computed for each of the ten microstates, from the averaged ERP map series of each subject and both prestimulus classes, using the microstate borders in Table 1. Since the microstate segment borders varied somewhat between subjects, the first and last 15% of the maps of each microstate were skipped for the computation of the microstate mean maps. The topography of the landscape of each of the mean maps was assessed numerically by the locations of the points of gravity of the positive and negative map area ("centroids", Wackermann et al., 1993, Appendix B) within the schematized electrode array (Fig. 1A) using electrode distance as unit of measurement. The map centroids reduce the map topography to four parameters, the locations of the positive and the negative centroid on the anterior-posterior and on the left-right axis; this characterization of the landscape is independent from the strength of the field. An example is illustrated in Fig. 1D.

Statistics

The four measures of map topography (the centroid locations) of each of the ten post-stimulus microstates were tested for differences between the two prestimulus microstate classes with repeated-measure 2-way MANOVAs (2 prestimulus map classes, 2 centroids [positive and negative] with the 2 dimensions [left-right and anterior-posterior] as the variate consisting of two dependent variables); the main effects of centroid polarity in the MANOVAs are of no interest in the present study and therefore are not reported. Paired t-tests were used to examine class effects on each centroid and dimension. Two-tailed p values are reported.

Results

The mean maps of the ten ERP microstates were averaged over the two prestimulus classes and the twelve subjects; they are illustrated in Fig. 3. The mean locations of the landscape-describing positive and negative centroids of these microstates are shown in Fig. 4 for the two prestimulus map classes I and II. These pairs of the landscape-describing centroids of the ERP microstates were predominantly oriented in the anterior-posterior direction. This is reflected by the much larger variation of the mean centroid locations in the anterior-posterior dimension. The absolute values (in electrode distances) ranged (means across subjects) in the 10 microstates and the two centroid polarities and the two pre-stimulus classes from 3.07 to 7.05 for the anterior-posterior dimension (SD between 0.62 and 2.37), and from 3.3 to 4.63 for the left-right dimension (SD between 0.16 and 0.94). The topographic relation between the two prestimulus classes, i.e., their differing field orientations appeared to be reflected in the post-stimulus microstates #2 and #5, but not in

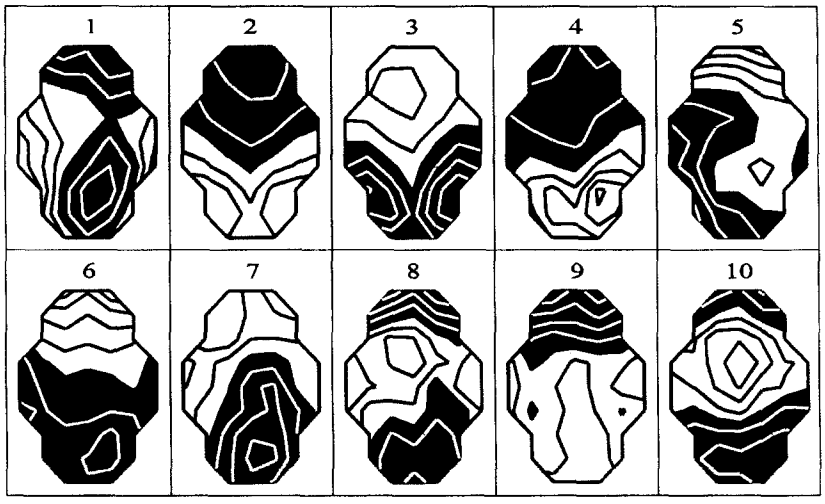

Fig. 3. Equipotential contour-line maps of the grand mean potential distribution of the ten microstates. Black negative, white positive referred to average reference. Head seen from above, nose up, left ear left. Equipotential-lines in steps of 0.5 microVolt. For the electrode arrangement see Fig. 1A

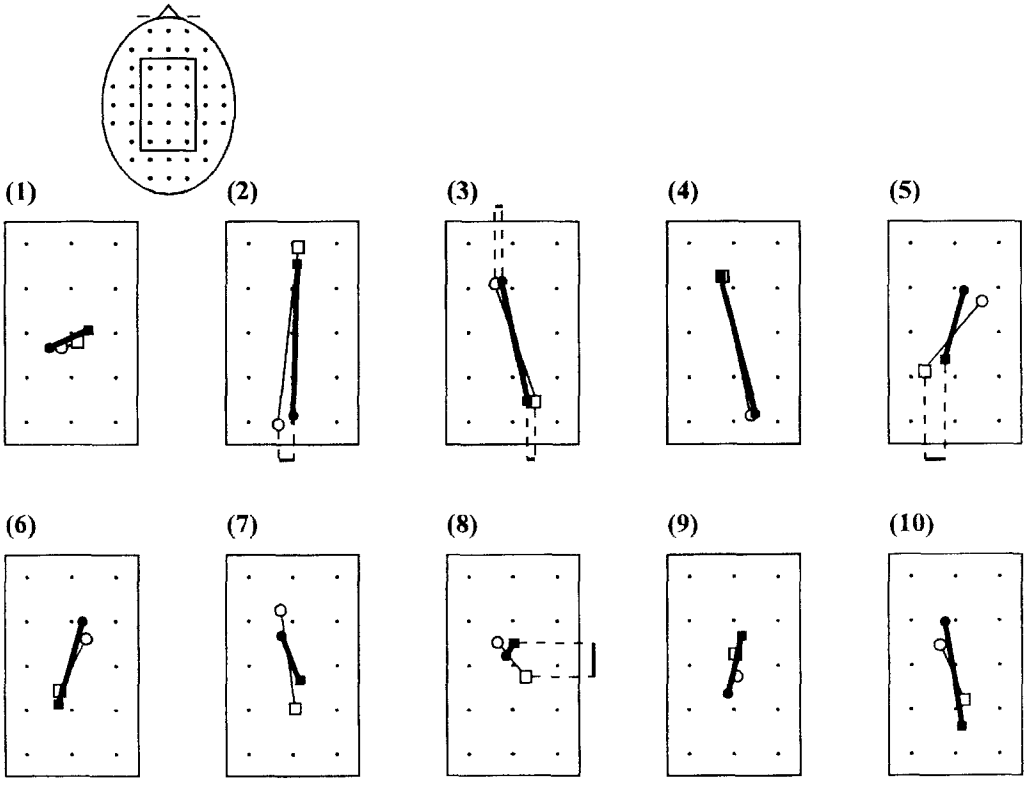

Fig. 4. Mean locations across subjects of the positive centroids (round symbols) and negative centroids (square symbols) of the maps of the ten microstates of the two prestimulus classes. The centroids of each class are connected by a line for easier viewing (class I: filled symbols and heavy line; class II: open symbols and thin line). T-test differences at $p < 0.05$ between microstate centroid locations of the two prestimulus classes are indicated by dotted lines and bars. The illustrated area is only a portion of the entire recording area as shown in the inset. Head seen from above, nose up

Table 1. Time of onset and duration of the ten post-stimulus ERP microstates in msec. Values of $p < 0.02$ are listed for the repeated-measure 2-way MANOVAs (2 prestimulus map classes ×2 centroids [positive and negative] with the 2 dimensions [left-right and anterior-posterior] forming the variate). Only the main effects of class are reported, because the main effects of centroid polarity are of no interest in the present study. Values of $p < 0.20$ are listed for the t-tests comparing the landscape descriptors (locations of the negative and positive centroids) of the two prestimulus class-dependent post-stimulus ERP microstate maps

Microstate#	#1	#2	#3	#4	#5	#6	#7	#8	#9	#10
Time msec	25	61	131	193	291	338	439	490	568	615	674
Duration msec	36	70	62	98	47	101	51	78	47	59	
MANOVAs:										
Main effect of class	–	.17	.14	–	–	–	–	***.042***	–	–
Interaction class x polarity	–	.10	***.034***	–	**.09**	–	–	**.06**	–	–
T-Tests:										
NEG. CENTROID L-R	–	–	***.019***	–	***.017***	–	–	–	–	–
NEG. CENTROID A-P	–	–	–	–	–	–	**.08**	***.004***	–	.14
POS. CENTROID L-R	–	***.028***	***.009***	–	**.09**	–	–	–	–	–
POS. CENTROID A-P	–	–	–	–	–	.17	.20	.15	–	.18

microstate #3 which showed an inverted relation and not in microstate #8 which involved anterior-posterior differences.

The statistical tests of microstate landscape differences as function of the two prestimulus classes showed the following: The MANOVA results (Table 1) for microstates #3 (131–193 ms) and #8 (490–568 ms) yielded p-values for main effect or interactions of $p < 0.05$. Note that main effects as well as interactions in the MANOVA are direct indicators of differences in map topography; whether a main effect or an interaction is found depends on whether the positive and the negative centroid are affected in the same way or not. The detailed testing of the individual topography features (t-tests of Table 1) showed that the difference for microstate #3 consisted of significant left-right location differences of the anterior (positive) as well as of the posterior (negative) centroids for the two prestimulus classes. In microstate #8, the anterior-posterior dimension showed a very significant difference for the negative centroid. In addition, microstate #5 at 291–338 ms yielded statistical trends for landscape differences in the MANOVA; the t-tests revealed a significant left-right difference for the occipital (negative) centroid and a statistical trend for the anterior (positive) centroid; we note that these differences of relative orientation in microstate #5 were opposite in direction to those in microstate #3, and reflected the relative orientation of their respective prestimulus classes. The prestimulus class was also reflected in microstate #2 as supported by a significant L-R difference in the t-test.

Discussion

The present results give further support to the observation that the spatial configuration of the sub-second microstate that immediately precedes a stimulus affects the post-stimulus ERP maps (Lehmann et al., 1994). In the present analysis, the entire post-stimulus epoch was analyzed by parsing the ERP map series into microstates (Lehmann, 1987; Pascual-Marqui et al., 1995). Microstate #2 showed the expected posterior positive-anterior negative configuration that is typical of the P100 component in visual pattern stimulation (Lehmann and Skrandies, 1980; Brandeis et al., 1995).

The previous study on prestimulus microstate effects (Lehmann et al., 1994) had examined selected post-stimulus epochs (acoustic modality); the main result had been that the third post-stimulus analysis epoch (at 280–380 ms) significantly reflected the prestimulus differences; this could be seen as a continuation of the prestimulus landscape configuration. In fact, a similar result was seen in the present (visual modality) study during a corresponding time range, where microstate #5 at 291–338 ms significantly reflected the relative field orientations of the prestimulus classes, and the subsequent microstate #6 (338–439 ms) again showed a similar (but non-significant) effect. On the other hand, during a time range that was not analyzed in the previous study, the present ERP microstate #3 at 131–193 ms differed significantly in landscape as function of the prestimulus microstate; it showed a reversal of the orientation of the associated prestimulus microstate landscapes, contrary to microstate #5. Thus, the assumption that the prestimulus

configuration simply persists over an extended post-stimulus time or that only one type of dependent configuration persists during the ERP can be ruled out in the present analysis.

On the other hand, it is interesting that microstates #5 and #6 (291–338 ms and 338–439 ms) of the present visual modality-study showed similar differences as the third microstate that covered an about corresponding time range (280–380 ms) in the previous acoustic modality-study (Lehmann et al., 1994). Considering that the stimulus modality, the paradigm and the task differed in addition to some differences in details of the analysis, the related effect of the comparable prestimulus classes on the maps in the P300 time range in the two studies suggests that the prestimulus microstate configuration might excert an invariant modulating effect on the ERP map landscapes during this time.

The present results extend and specify the observation of a general state-dependency of input treatment as investigated in the frequency-domain studies reviewed in Introduction. Our present study concerned the functional importance of the brain electric microstates in the sub-second range (Lehmann, 1992). The results confirmed the observation that the spatial pattern of the microstate at stimulus arrival contributes crucially to the determination of the neuronal populations that are activated and produce the event-related potential map series. Accepting the assumption that the activity of different neural populations implies different functions, this suggests that the processing of information will differ as a function of the momentary brain microstate at information arrival, i.e., that the global brain state with its continual changes in the sub-second range plays an important role in information processing. This further implies that the variance of averaged event-related potential maps as well as that of behavioral responses might be reduced by taking into consideration the momentary microstate that exists at stimulus presentation.

Acknowledgements

Dr. I. Kondakor was supported by post-doctoral fellowships from The KEY Foundation for Brain-Mind Research, Zurich and from the Swiss National Science Foundation; he was on leave from his home Institution, the Department of Neurology, Medical School, University of Pécs, Hungary.

References

Ashby WR (1960) Design for a brain. Chapman & Hall, London

Basar E (1980) EEG brain dynamics. Elsevier, Amsterdam

Basar E, Basar-Eroglu C, Rosen B, Schutt A (1984) A new approach to endogenous event-related potentials in man: relation between EEG and P300-wave. Int J Neurosci 24: 1–21

Brandeis D, Lehmann D, Michel CM, Mingrone W (1995) Mapping event-related brain potential microstates to sentence endings. Brain Topogr 8: 145–159

Courchesne E (1978) Neurophysiological correlates of cognitive development: changes in long-latency event-related potentials from childhood to adulthood. Electroencephalogr Clin Neurophysiol 45:468–482

Corletto F, Gentilomo A, Rosadini A, Rossi GF, Zattoni J (1967) Visual evoked responses during sleep in man. Electroencephalogr Clin Neurophysiol [suppl] 26: 61–69

Friedman D, Putnam L, Sutton S (1990) Longitudinal and cross-sectional comparisons of young children's cognitive ERPs and behavior in a picture-matching task: preliminary findings. Int J Psychophysiol 8: 213–221
Gath I, Lehmann D, Bar-On E (1983) Fuzzy clustering of EEG signal and vigilance performance. Int J Neurosci 20: 303–312
Gath I, Bar-On E, Lehmann D (1985) Automatic classification of visual evoked responses. Comput Methods Programs Biomed 20: 17–22
John ER, Prichep LS, Fridman J, Easton P (1988) Neurometrics: computer-assisted differential diagnosis of brain dysfunctions. Science 239: 162–169
Kinoshita T, Strik WK, Michel CM, Yagyu T, Saito M, Lehmann D (1995) Microstate segmentation of spontaneous multichannel EEG map series under diazepam and sulpiride. Pharmacopsychiatry 28: 51–55
Koelega HS, Verbaten MN (1991) Event-related brain potentials and vigilance performance: dissociations abound, a review. Percept Mot Skills 72: 971–982
Koenig T (1995) Brain electric microstates and the processing of language. Thesis, Swiss Federal Institute of Technology, Zurich (Nr. 11153)
Koenig T, Lehmann D (1996) Microstates in language-related brain potential maps show noun-verb differences. Brain Lang 53: 169–182
Kondakor I, Pascual-Marqui RD, Michel CM, Lehmann D (1995) Event-related potential map differences depend on the prestimulus microstates. J Med Eng Technol 19: 66–69
Koukkou M, Lehmann D (1968) EEG and memory storage in sleep experiments with humans. Electroencephalogr Clin Neurophysiol 25: 455–462
Koukkou M, Lehmann D (1983) Dreaming: the functional state-shift hypothesis. Br J Psychiatry 142: 221–231
Kutas M, Hillyard SA (1980) Reading senseless sentences: brain potentials reflect semantic incongruity. Science 207: 203–205
Lehmann D (1971) Multichannel topography of human alpha EEG fields. Electroencephalogr Clin Neurophysiol 31: 439–449
Lehmann D (1987) Principles of spatial analysis. In: Gevins AS, Remond A (eds) Handbook of electroencephalography and clinical neurophysiology, vol 1. Methods of analysis of brain electrical and magnetic signals. Elsevier, Amsterdam, pp 309–354
Lehmann D (1992) Brain electric fields and brain functional states. In: Friedrich R, Wunderlin A (eds) Evolution of dynamical structures in complex systems. Springer, Berlin Heidelberg New York Tokyo, pp 235–248
Lehmann D, Skrandies W (1980) Reference-free identification of components of checkerboard-evoked multichannel potential fields. Electroencephalogr Clin Neurophysiol 48: 609–621
Lehmann D, Ozaki H, Pal I (1987) EEG alpha map series: brain electric micro-states by space-oriented adaptive segmentation. Electroencephalogr Clin Neurophysiol 67: 271–288
Lehmann D, Michel CM, Pal I, Pascual-Marqui RD (1994) Event-related potential maps depend on prestimulus brain electric microstate map. Int J Neurosci 74: 239–248
McCallum WC (1988) Potentials related to expectancy, preparation and motor activity. In: Picton W (ed) Handbook of electroencephalography and clinical neurophysiology, vol 3. Human event-related potentials. Elsevier, Amsterdam, pp 427–459
Michel CM, Lehmann D (1993) Single doses of piracetam affect 42-channel event-related potential microstate maps in a cognitive paradigm. Neuropsychobiology 28: 212–221
Näätänen R, Paavilainen P, Tiitinen H, Jiang D, Alho K (1993) Attention and mismatch negativity. Psychophysiology 30: 436–450
Offner FF (1950) The EEG as potential mapping: the value of the average monopolar reference. Electroencephalogr Clin Neurophysiol 2: 215–216
Oldfield RC (1970) The assesment and analysis of handehness: the Edinburgh inventory. Neuropsychologia 9: 97–113

Pascual-Marqui RD, Michel CM, Lehmann D (1995) Segmentation of brain electrical activity into microstates: model estimation and validation. IEEE Trans Biomed Eng 42: 658–665

Picton TW (1992) The P300 wave of the human event-related potential. J Clin Neurophysiol 9: 456–479

Rahn E, Basar E (1993) Enhancement of visual evoked potentials by stimulation during low prestimulus EEG stages. Int J Neurosci 72: 123–136

Romani A, Callieco R, Cosi V (1988) Prestimulus spectral EEG patterns and the evoked auditory vertex response. Electroencephalogr Clin Neurophysiol 70: 270–272

Romani A, Bergamaschi R, Callieco R, Cosi V (1991) Prestimulus EEG influence on late ERP components. Boll Soc Ital Biol Sper 67: 77–82

Takeda M, Tachibana H, Sugita M, Hirayama H, Miyauchi M, Matsuoka A (1992) Event-related potential in patients with diabetes mellitus. Rinsho Byori 40: 896–900

Wackermann J, Lehmann D, Michel CM, Strik WK (1993) Adaptive segmentation of spontaneous EEG map series into spatially defined microstates. Int J Psychophysiol 14: 269–283

Woods DL, Alho K, Algazi A (1993) Intermodal selective attention: evidence for processing in tonotopic auditory fields. Psychophysiology 30: 287–295

Authors' address: Dr. I. Kondakor, The KEY Institute for Brain-Mind Research, University Hospital of Psychiatry, Lenggstrasse 31, CH-8029 Zurich, Switzerland.

Received April 22, 1996